DYNAMICS OF TERNARY MICROEMULSIONS

Shigeyuki Komura
Department of Mechanical System Engineering,
Faculty of Computer Science and Systems Engineering,
Kyushu Institute of Technology, Iizuka 820, Japan

Hiroya Kodama
Mitsubishi Chemical Corporation, Research and Development Division,
Yokohama Research Center, Yokohama 227, Japan

Dynamics of microphase separation of an oil-water-surfactant system is investigated by means of cell dynamical system approach on the basis of newly proposed two-order-parameter time dependent Ginzburg-Landau model. For equal volumes of oil and water, the time evolution of characteristic length scale of domains is investigated by changing the average surfactant concentration. The more the amount of surfactant, the slower the dynamics. The results are analyzed by using the crossover scaling assumption. Dynamic response of microemulsions to shear deformation is also investigated. Time evolution of anisotropic factor under steady shear flow is studied by changing shear rate and total amount of surfactant. As the surfactant concentration is increased, overshoot peak height of the anisotropic factor increases.

1 Introduction

Microemulsions being mixture of oil, water and surfactant are known to exhibit various interesting microstructures depending on the temperature or the composition (1). When the concentration of surfactant is relatively large, they show a rich variety of regularly ordered structures such as the cubic phase, the hexagonal phase or the lamellar phase. By lowering the concentration of surfactant and if the volumes of oil and water are not very different, microemulsions form a bicontinuous structure where a multiply connected randomly oriented monolayer of surfactants separate oil-rich and water-rich subvolumes with a mesoscopic length scale ($10 \sim 100$nm).

There are several experimental evidences for the convoluted structure of oil and water such as by measuring the conductivity (2) or the diffusivities of molecules (3). A direct observation of the randomly intertwined structure by using the freeze-fracture microscopy has been also reported (4). Several X-ray and neutron scattering experiments showed that the structure factor of the bicontinuous phase shows a peak at non-zero wavevector k indicating that there is a structure on a length scale $2\pi/k$ (5). It is also found that for microemulsions containing equal volumes of oil and water, the peak position shifts to

larger values of k and peak height diminishes as the surfactant concentration is increased (6).

When one quenches a ternary system from a high temperature homogeneous phase where the system is uniformly mixed to a low temperature phase where a certain structure appears, the average domain size increases in time until it reaches the equilibrium size. Since the surfactants act to lower the interfacial tension and the driving force for the phase separation is decreased, it is natural to expect that the dynamics of domain growth becomes significantly slower in the presence of surfactants. With this perspective, several people have investigated the effect of added surfactants on the phase separation dynamics using different models. For instance, Kawakatsu *et al.* have proposed a "hybrid model" where oil and water are represented by coarse-grained fields and surfactants are treated microscopically (7), whereas Laradji *et al.* performed molecular dynamics simulations (8). Both of these works have shown that the system containing surfactants exhibits a slow non-algebraic growth of the domains, in contrast to the pure binary systems.

Qualitatively same results have been also reported in the other paper by Laradji and his coworkers who proposed a phenomenological two-order-parameter Ginzburg-Landau free energy associated with standard time dependent Ginzburg-Landau (TDGL) equations (9). In their model, one of the order parameters represents the local concentration difference between oil and water, while the other one represents the local surfactant concentration. Recently, Pätzold and Dawson extended the model by Laradji *et al.* to incorporate the hydrodynamic effects by coupling the TDGL equations to Navier-Stokes-type equations (10). They found that, in the presence of the hydrodynamic interactions, the crossover scaling exponent becomes different from that obtained by Laradji *et al* (9).

However, it is criticized in the book by Gompper and Shick that the two-order-parameter model by Laradji *et al.* is not well-defined, since the free energy of configurations with large surfactant concentration at the oil/water interfaces is not bounded from below (1). So far, quite general expression of two-order-parameter Ginzburg-Landau model has been given also by Gompper and Shick (1). In fact, the model by Laradji *et al.* can be considered as one of the special cases of their expression with too much simplification. Because of the above reasons, the quantitative study on the phase separation dynamics based on the well-defined two-order-parameter model has not yet been done.

Another aspect of the dynamics of microemulsions is related to the structural change in response to externally applied perturbations. The rheological properties of microemulsions has been theoretically investigated by Mundy *et al.* using a single-order-parameter TDGL model (11) and later extended by

Pätzold and Dawson who also performed computer simulations (12). Here the only order parameter describes the concentration difference between oil and water and the presence of surfactants is taken into account through surface tension parameter. (This point will be discussed later.) In Ref. (12), authors showed that the microemulsions behave in an essentially non-Newtonian manner. As discussed in the paper by Pätzold and Dawson (12), the next step in the computational study of the rheology of microemulsions is to include the surfactant concentration field. Generally speaking, for a ternary mixture, it is natural to characterize the system in terms of two independent concentration variables.

In the this paper, we shall propose a new minimum two-order-parameter Ginzburg-Landau model in which the above problems are removed but still expresses the essential features of the ternary system. Our model intrinsically includes the preferred value of the surfactant concentration when surfactant molecules aggregate. Moreover we required in our model that when surfactants aggregate at the interface, the interfacial tension becomes very small. Using the proposed model, we numerically study the dynamics of phase separation (13) and also investigate the dynamic response of microemulsions to shear deformation (14). Here we pay attention to the case where the volumes of oil and water are equal.

This paper is constructed as follows. In Sec. 2, after reviewing the model by Laradji *et al.*, we present our model and discuss its physical meanings. In Sec. 3, we describe our simulation method which is essentially based on the cell dynamical system approach. Sec. 4 gives the results for the dynamics of phase separation, whereas Sec. 5 gives that for the dynamic response to shear deformation. This paper ends with discussions in Sec. 6.

2 Two-Order-Parameter Model

In this section, we shall first review the two-order-parameter model proposed by Laradji *et al.* (9). In their model, the local concentration difference between oil and water is described by $\psi(\boldsymbol{r})$ and the local surfactant concentration measured from a certain reference value is denoted as $\rho(\boldsymbol{r})$. Their model is

$$F_L = \int \mathrm{d}\boldsymbol{r} \left[d(\nabla\psi)^2 - a\psi^2 + u\psi^4 + b\rho^2 + g\psi^2\rho^2 - s\rho(\nabla\psi)^2 \right], \qquad (1)$$

where d, a, u, b, g and s are positive constants. The term $b\rho^2$ prevents the surfactants from forming clusters. The local coupling term $g\psi^2\rho^2$ guarantees that the local surfactant concentration remains small in the bulk where $|\psi|$ is large. The last non-local coupling term $-s\rho(\nabla\psi)^2$ favors the surfactants

to sit at oil/water interfaces. As mentioned in the introduction, however, this free energy functional is not bounded from below for positive values of s (1). Although Pätzold and Dawson reported that they did not find any numerical instabilities within the parameter values they used (10), we observed a diverging tendency of the surfactant concentration at the oil/water interfaces as we decreased the simulation mesh size. The finite value of ρ is supported only by the non-zero simulation mesh size. This is obviously not reasonable from the point of view of solving continuous partial differential equations. Moreover, we found that the domains do not flow globally in the presence of a convective macroscopic flow within their model. This problem also seems to be related to the model intrinsic singular behavior at the oil/water interfaces.

Here we propose a different two-order-parameter Ginzburg-Landau free energy functional which has no drawbacks mentioned above. What we have required in our model are that (i) the profiles of ψ and ρ at oil/water interfaces do not depend on the average values of ψ and ρ (denoted hereafter as $\overline{\psi}$ and $\overline{\rho}$, respectively) and that (ii) the coarse-graining dynamics of ψ based on the free energy becomes slow when the amplitude of ρ at the interface takes a certain saturated value. The newly proposed minimum model which fulfills these requirements is

$$F = \int \mathrm{d}r \left[w(\nabla^2\psi)^2 + d(\nabla\psi)^2 - a\psi^2 + u\psi^4 + e\rho^2(\rho-\rho_s)^2 - s\rho(\nabla\psi)^2 \right], \tag{2}$$

where w, d, a, u, e, ρ_s and s are positive constants. First we have added the term $w(\nabla^2\psi)^2$ which prevents the model from becoming unbounded. Next we replaced the local potential of ρ with a double-minimum potential $e\rho^2(\rho-\rho_s)^2$ which allows the coexistence of the two bulk states, i.e., $\rho = 0$ and $\rho = \rho_s$. The physical meaning of these two states are as follows. The state $\rho = 0$ corresponds to the case in which the system is locally occupied either by oil or water. There are no surfactants in the considered local volume. The state $\rho = \rho_s$ corresponds to the case in which the local volume is occupied only by surfactants. The quantity ρ_s can be considered to represent the density of condensed hydrocarbon chains of surfactants when they self-assemble. It is likely that in any type of surfactant aggregates, the density of hydrocarbon chains does not change appreciably. It should be noted here that we did not include any gradient term of ρ, say $(\nabla\rho)^2$. This is physically reasonable since the energy cost due to the direct attachment between hydrocarbon chains and oil molecules or between hydrophilic head and water molecules is small. As regards the coupling terms, the local coupling term $g\psi^2\rho^2$ in Eq. (1) has been dropped out, whereas only the non-local coupling term $-s\rho(\nabla\psi)^2$ is left here. Due to the latter term, the state with $\rho = \rho_s$ tends to occupy the narrow region

around the oil/water interfaces. It is also essential in microemulsions that the interfacial tension vanishes when the interface is saturated with surfactants (15; 16). For this reason, we chose the values of parameters to satisfy the relation $d = s\rho_s$, which plays an essential role for our requirement (ii) in the model. We believe that Eq. (2) is one of the minimum models which is sufficient to grasp the essential properties of microemulsions. Another possibility of the model will be discussed in the last section.

For the time evolution of $\psi(\boldsymbol{r}, t)$ and $\rho(\boldsymbol{r}, t)$, we assume the standard TDGL equations. Both ψ and ρ are conserved quantities. Since we later consider the case that there is a macroscopic flow $\boldsymbol{v}$, TDGL equations acquire a convective term and become

$$\frac{\partial \psi}{\partial t} + \nabla \cdot (\boldsymbol{v}\psi) = M_\psi \nabla^2 \frac{\delta F}{\delta \psi} + \eta_\psi(\boldsymbol{r}, t), \tag{3}$$

$$\frac{\partial \rho}{\partial t} + \nabla \cdot (\boldsymbol{v}\rho) = M_\rho \nabla^2 \frac{\delta F}{\delta \rho} + \eta_\rho(\boldsymbol{r}, t). \tag{4}$$

Here M_ψ and M_ρ are transport coefficients, and η_ψ and η_ρ represent thermal noise which satisfy the fluctuation-dissipation theorem: $\langle \eta_{\psi(\rho)}(\boldsymbol{r}, t)\eta_{\psi(\rho)}(\boldsymbol{r}', t')\rangle = -2k_B T M_{\psi(\rho)} \nabla^2 \delta(\boldsymbol{r} - \boldsymbol{r}')\delta(t - t')$, where k_B is the Boltzmann constant and T is the temperature. As regards the macroscopic flow in Eqs. (3) and (4), here we only consider a simple shear flow $v_x(\boldsymbol{r}) = \dot{\gamma} y, v_y = v_z = 0$, where the shear rate $\dot{\gamma}$ is the time derivative of the strain γ. By inserting Eq. (2) into Eqs. (3) and (4), the time evolution equations can be explicitly written as

$$\begin{aligned} \frac{\partial \psi}{\partial t} &= -\dot{\gamma} y \frac{\partial \psi}{\partial x} + M_\psi \nabla^2 \left[-2a\psi + 4u\psi^3 + 2w\nabla^4 \psi \right. \\ &\quad \left. -2(d - s\rho)\nabla^2 \psi + 2s(\nabla \psi) \cdot (\nabla \rho) \right] + \eta_\psi(\boldsymbol{r}, t), \end{aligned} \tag{5}$$

$$\frac{\partial \rho}{\partial t} = -\dot{\gamma} y \frac{\partial \rho}{\partial x} + M_\rho \nabla^2 \left[2e\rho(\rho - \rho_s)(2\rho - \rho_s) - s(\nabla \psi)^2 \right] + \eta_\rho(\boldsymbol{r}, t). \tag{6}$$

In the present work, we have entirely ignored the hydrodynamic interactions which might play an important role in microemulsions. One of the realistic systems which corresponds to our model is a binary homopolymer mixture containing diblock copolymers (17). Since we have not included the hydrodynamic interactions, our model lacks a bare viscous time scale. Nevertheless, we can chose the model intrinsic time scale as the inverse of the initial growth rate of the most unstable mode. The wavevector dependent initial growth rate is defined as

$$\frac{\partial \psi_{\boldsymbol{k}}(t)}{\partial t} = \Lambda(\boldsymbol{k})\psi_{\boldsymbol{k}}(t), \tag{7}$$

where we have introduced the spatial Fourier transform of $\psi(\boldsymbol{r},t)$ as $\psi_{\boldsymbol{k}}(t) = \int \mathrm{d}\boldsymbol{r}\psi(\boldsymbol{r},t)\exp(i\boldsymbol{k}\cdot\boldsymbol{r})$. Since the typical time scale for surfactants to assemble at the oil/water interfaces is long compared to that of initial phase ordering process, we neglect here the effect of surfactants on $\Lambda(\boldsymbol{k})$. Hence we have

$$\Lambda(k) = -2M_\psi(wk^6 + dk^4 - ak^2), \tag{8}$$

where $k = |\boldsymbol{k}|$. The most unstable mode $k = k_0$ which maximizes $\Lambda(\boldsymbol{k})$ is

$$k_0^2 = \frac{-d + \sqrt{d^2 + 3aw}}{3w}. \tag{9}$$

Thus the typical time scale τ_0 in our model is given by $\tau_0 = 1/\Lambda(k_0)$.

3 Cell Dynamical System Approach

In order to solve the above time evolution equations, we used the cell dynamical system (CDS) approach proposed by Oono *et al.* (18). The CDS model is a space-time discrete model to describe a phenomena at the mesoscopic level and proved to be an efficient algorithm for numerical simulations. Here we restricted ourselves to a two-dimensional system. Accordingly, the space coordinate is specified by the lattice point $\boldsymbol{n} = (n_x, n_y)$ in an $L \times L$ square lattice. We also impose periodic boundary conditions. The CDS equations corresponding to Eqs. (5) and (6) are

$$\psi(\boldsymbol{n},t+1) = \psi(\boldsymbol{n},t) - \dot{\gamma}n_y\tilde{\partial}_x\psi(\boldsymbol{n},t) + M_\psi\tilde{\nabla}^2\mathcal{I}(\boldsymbol{n},t) + C_\psi\eta(\boldsymbol{n},t), \tag{10}$$

$$\rho(\boldsymbol{n},t+1) = \rho(\boldsymbol{n},t) - \dot{\gamma}n_y\tilde{\partial}_x\rho(\boldsymbol{n},t) + M_\rho\tilde{\nabla}^2\mathcal{J}(\boldsymbol{n},t) + C_\rho\eta'(\boldsymbol{n},t), \tag{11}$$

where $\mathcal{I}(\boldsymbol{n},t)$ and $\mathcal{J}(\boldsymbol{n},t)$ are the discrete thermodynamic forces given by

$$\mathcal{I}(\boldsymbol{n},t) = -A\tanh\psi + \psi + W(\tilde{\nabla}^2)^2\psi - (D - S\rho)\tilde{\nabla}^2\psi + S(\tilde{\nabla}\psi)\cdot(\tilde{\nabla}\rho), \tag{12}$$

$$\mathcal{J}(\boldsymbol{n},t) = E\rho(\rho-\rho_s)(2\rho-\rho_s) - \frac{1}{2}S(\tilde{\nabla}\psi)^2, \tag{13}$$

respectively. The "tanh" term in Eq.(12) is introduced for the sake of numerical stability (18). In the above equations, the discretized differential operators are defined as $\tilde{\nabla}\phi = (\tilde{\partial}_x\phi, \tilde{\partial}_y\phi) = \frac{1}{2}[\phi(n_x+1,n_y) - \phi(n_x-1,n_y), \phi(n_x,n_y+1) - \phi(n_x,n_y-1)]$ and $\tilde{\nabla}^2\phi = (1/2)\sum\phi$(nearest-neighbor cells) $+ (1/4)\sum\phi$(next-nearest-neighbor cells) $- 3\phi$, respectively. (ϕ denotes either ψ or ρ.) The noise terms in Eqs. (10) and (11) are given by $\eta^{(\prime)}(\boldsymbol{n},t) = \eta_x^{(\prime)}(n_x+1,n_y,t) - \eta_x^{(\prime)}(n_x,n_y,t) + \eta_y^{(\prime)}(n_x,n_y+1,t) - \eta_y^{(\prime)}(n_x,n_y,t)$, where $\eta_x^{(\prime)}$

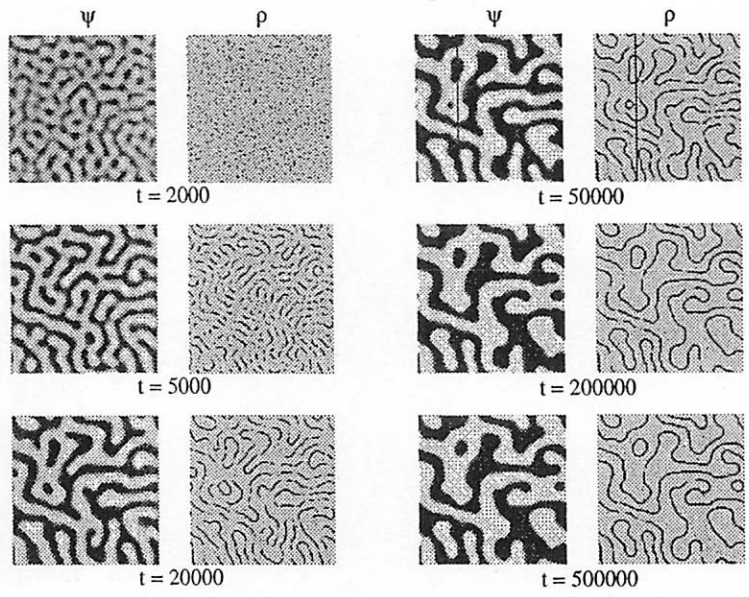

Figure 1: Time evolutions of ψ and ρ for $\overline{\rho} = 0.1$. The left and right column shows the spatial distribution of ψ and ρ fields, respectively. Dark area denotes the region of higher values of ψ and ρ. Notice that the typical time scale is $\tau_0 \approx 5.0 \times 10^2$.

and $\eta_y^{(\prime)}$ are random numbers uniformly distributed in the interval $[-1, 1]$ and $C_{\psi(\rho)}$ are the noise amplitudes taken as independent parameters in CDS (19). The noise perturbations are important in order to accelerate the evolution processes and prevent domains from freezing (10).

In our simulations, we fixed the parameters to $L = 128$, $A = 1.3$, $W = 0.2$, $D = 0.5$, $S = 0.5$, $E = 0.25$, $\rho_s = 1$, $M_\psi = M_\rho = 0.05$, $C_\psi = C_\rho = 0.02$ and $\overline{\psi} = 0$, whereas $\overline{\rho}$ has been changed as $\overline{\rho} = 0.1, 0.2, 0.3, 0.4$ and 0.5. Notice that our parameter choice satisfies $D = S\rho_s$ which ensures the interfacial tension to vanish when $\rho = \rho_s$. The initial distributions of ψ and ρ are specified by a random uniform distribution in the range $[\overline{\psi} - 0.01, \overline{\psi} + 0.01]$ and $[\overline{\rho} - 0.01, \overline{\rho} + 0.01]$, respectively. With our choice of parameters, the most unstable mode is $k_0 \approx 0.51$ (Eq. (9)) and the typical time scale is $\tau_0 \approx 5.0 \times 10^2$.

In the presence of the shear flow, we required a boundary condition such that $\phi(n_x, n_y, t) = \phi(n_x + iL + \gamma jL, n_y + jL, t)$ holds for arbitrary integers i and j (20). Before the shear flow is applied, Eqs. (10) and (11) are numerically solved up to 5×10^5 time steps. After this process, we apply the shear flow with $\dot{\gamma} = 2 \times 10^{-4}$, 5×10^{-4}, 1×10^{-3} and 2×10^{-3}. In Sec. 5, the time origin is taken as the instance when the shear flow is turned on. Notice that the investigated shear ranges from the weak to the medium shear ($\dot{\gamma}\tau_0 = 0.1 \sim 1$).

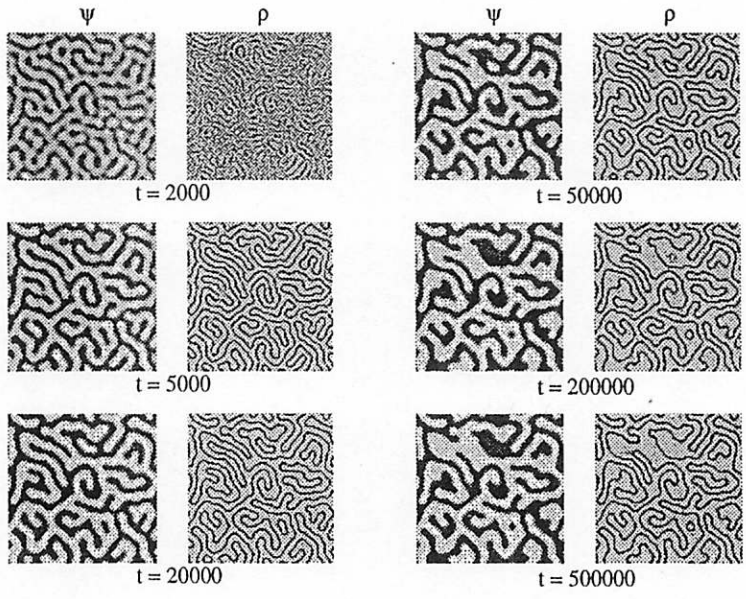

Figure 2: Time evolutions of ψ and ρ for $\overline{\rho} = 0.4$. The same with Fig.1.

4 Dynamics of Phase Separation

In this section, we discuss the result of the dynamics of phase separation in the absence of shear flow, i.e., $\dot{\gamma} = 0$. The typical time evolutions of ψ and ρ are depicted in Figs. 1 and 2 for $\overline{\rho} = 0.1$ and $\overline{\rho} = 0.4$, respectively. For a quantitative discussion, we have calculated the average domain size of ψ in the following way. First a discrete Fourier transform of $\psi(\boldsymbol{n}, t)$ is defined by $\psi_{\boldsymbol{k}}(t) = \sum_{\boldsymbol{n}} \psi(\boldsymbol{n}, t) \exp(i\boldsymbol{k} \cdot \boldsymbol{n})$ with $\boldsymbol{k} = 2\pi \boldsymbol{n}/L$ and $\boldsymbol{n} \in \{0, 1, \cdots, L-1\}^2$. The structure factor is given by $S(\boldsymbol{k}, t) = \langle \psi_{\boldsymbol{k}}(t) \psi_{-\boldsymbol{k}}(t) \rangle$, where the average is over the ensemble of systems. In this paper, we calculated the time dependent (inverse) characteristic length scale defined by (21)

$$\langle k(t) \rangle = \frac{\sum_{\boldsymbol{k} \neq \boldsymbol{0}} |\boldsymbol{k}|^{-1} S(\boldsymbol{k}, t)}{\sum_{\boldsymbol{k} \neq \boldsymbol{0}} |\boldsymbol{k}|^{-2} S(\boldsymbol{k}, t)}. \tag{14}$$

This expression provides better estimation of the characteristic length scale than that obtained by using the spherically averaged structure factor (21). In Fig. 3, $\langle k(t) \rangle$ is plotted as a function of time step for different values of $\overline{\rho}$ for the noiseless case ($C_\psi = C_\rho = 0$). Each line corresponds to a single run. By turning off the coupling between ψ and ρ, we have also included the result of ordinary spinodal decomposition which exhibits the well-known $t^{-1/3}$ evolution. The estimated most unstable mode k_0 is consistent with our simulation result. We recover the following features which have been also found in the previous works. (i) In the presence of surfactants, evolution of the pattern becomes exceedingly

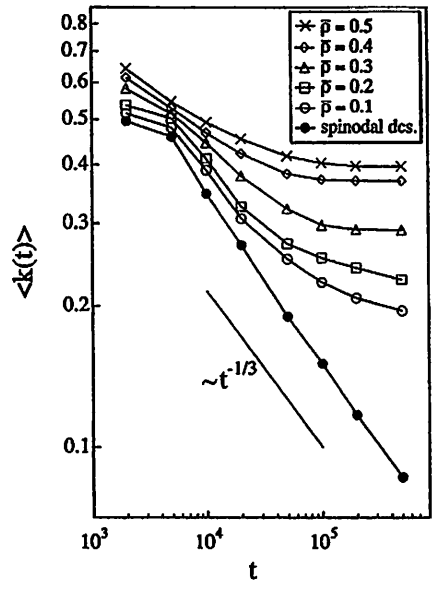

Figure 3: Inverse characteristic length scale $\langle k(t) \rangle$ as a function of time step for different values of $\overline{\rho}$. The straight line has a slope of $-1/3$.

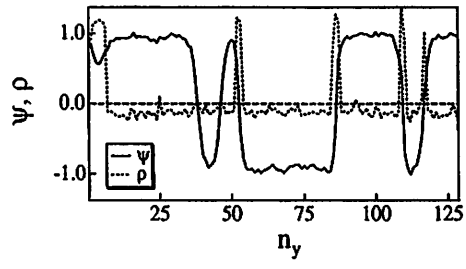

Figure 4: Profiles of ψ and ρ along the straight lines drawn in Fig. 1 (a) ($t = 50000$). The solid line represents ψ and dashed line represents ρ.

slow, which appears to be almost logarithmic in time for large time steps and large $\overline{\rho}$. (ii) At almost any time step, the average domain size decreases as $\overline{\rho}$ is increased.

In addition to these features, especially for small $\overline{\rho}$, we can observe the coexistence of two types of interfaces at the early stage of phase separation, *i.e.* the coexistence of saturated interface and unsaturated interface. At the saturated interfaces, ρ takes a saturated value (slightly above 1), whereas the value of ρ at the unsaturated interfaces is almost the same as that in the balk phase. This can be more clearly seen in Fig. 4 where we plotted the cross section profiles of the two fields along the straight lines drawn in Fig. 1 ($t = 50000$). As the phase separation proceeds, the system will eventually be governed by the saturated interfaces and will reach the equilibrium configuration. It is interesting to note that the dynamics of phase separation in microemulsions

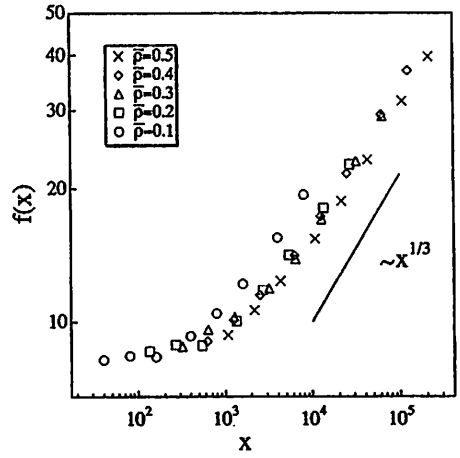

Figure 5: Scaling plot of $f(x)$ as a function of x. The straight line has a slope of 1/3.

can be understood from the point of view of motion of one-dimensional interface (or contour) separating saturated and unsaturated interfaces.

The time evolution of the characteristic length scale for various values of $\overline{\rho}$ has been analyzed by using the crossover scaling assumption. Since the hydrodynamic interaction is ignored in our simulation, we consider a similar form proposed in Ref. (9);

$$\langle k(t) \rangle = t^{-1/3} f((\overline{\rho} - \rho_0)^3 t), \tag{15}$$

where $f(x)$ is a scaling function with $f(x) \sim$ const. for $x \to 0$ and $f(x) \sim x^{1/3}$ for $x \to \infty$. Here, we denote the average value of ρ in the bulk phase as ρ_0, which can be considered to correspond to the origin of the surfactant density. We checked that this value does not depend on $\overline{\rho}$. Hence for small x, the characteristic length scale exhibits a $t^{-1/3}$ behavior as in the ordinary spinodal decomposition, whereas for large x, it becomes proportional to the total surfactant concentration. The latter fact has been confirmed both by experiments (6) and by Monte Carlo simulations (22) and can be interpreted in the following way; if all the interfaces are saturated, the total amount of surfactant should be proportional to the total area ("length" in our simulation) of the interface which is also proportional to the inverse characteristic length. In Fig. 5, we have plotted the scaling function $f(x)$ as a function of x for various values of $\overline{\rho}$ by fixing $\rho_0 = -0.1$. Although the data collapse for larger values of $\overline{\rho}$ is satisfactory, the data for small $\overline{\rho}$ (such as $\overline{\rho} = 0.1$) deviate slightly from the universal behavior.

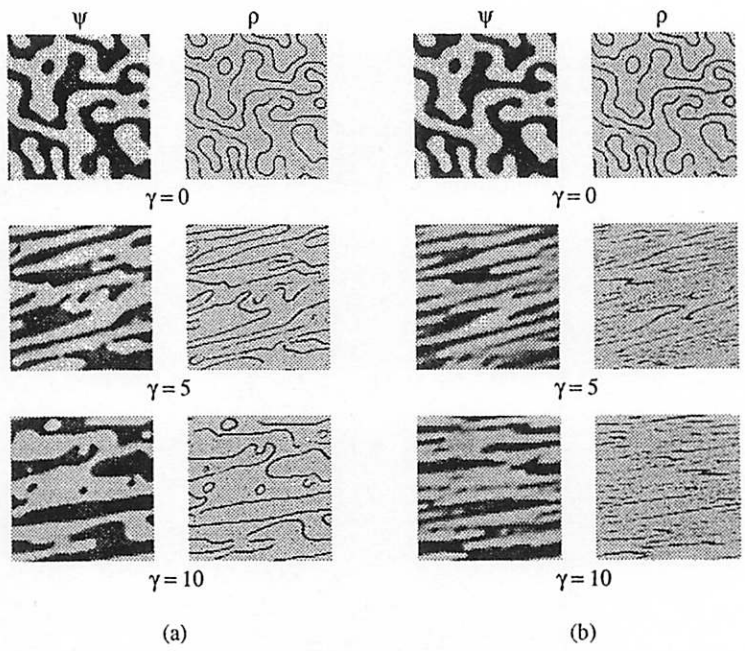

Figure 6: Time evolution of ψ (left) and ρ (right) for (a) $\overline{\rho} = 0.1$, $\dot{\gamma} = 2 \times 10^{-4}$ ($\dot{\gamma}\tau_0 = 0.1$) and (b) $\overline{\rho} = 0.1$, $\dot{\gamma} = 2 \times 10^{-3}$ ($\dot{\gamma}\tau_0 = 1$).

5 Response to Shear Flow

In this section, we discuss the dynamical response to the steady shear flow with non-zero $\dot{\gamma}$. Typical time evolutions of ψ and ρ are shown in Fig. 6 for (a) $\overline{\rho} = 0.1$, $\dot{\gamma} = 2 \times 10^{-4}$ ($\dot{\gamma}\tau_0 = 0.1$) and (b) $\overline{\rho} = 0.1$, $\dot{\gamma} = 2 \times 10^{-3}$ ($\dot{\gamma}\tau_0 = 1$). By changing $\overline{\rho}$ and $\dot{\gamma}$, we found the following general behaviors. When the shear rate is small, surfactants move under the flow keeping themselves attached to the oil/water interfaces. The total amount of the interface does not seem to change appreciably during the deformation. On the other hand, when the shear rate is large, some surfactants are blown off the interfaces by the shear. The coagulation and break-up processes take place as has been observed in the spinodal decomposition under steady shear flow (20) and the total amount of the interface increases.

Given the evolving patterns, we have evaluated the anisotropic factor defined by (11; 12)

$$Q_{xy} = \frac{1}{\Omega} \sum_{n} \left[-D(\tilde{\partial}_x \psi)(\tilde{\partial}_y \psi) - 2W(\tilde{\partial}_x \tilde{\partial}_y \psi)(\tilde{\nabla}^2 \psi) \right], \tag{16}$$

where Ω is the total volume (area) of the system. Although this quantity essentially represents the xy-component of the macroscopic excess stress tensor in the case of spinodal decomposition without any surfactants (20), this is not the case in the present model since there should be a contribution to the stress

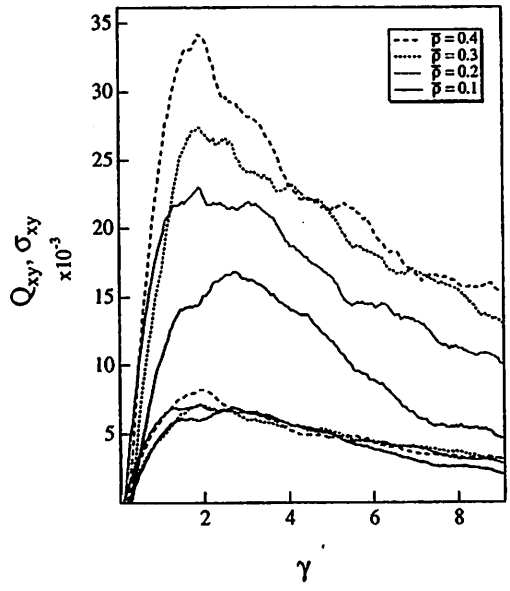

Figure 7: Q_{xy} (upper 4 curves, see Eq. (10)) and σ_{xy} (lower 4 curves, see Eq. (11)) as a function of the shear strain $\gamma = \dot{\gamma}t$ for fixed $\dot{\gamma} = 2 \times 10^{-4}$ and $\overline{\rho} = 0.1$, 0.2, 0.3, 0.4.

due to the non-local coupling term in Eq. (2). Here we propose here the following quantity

$$\sigma_{xy} = \frac{1}{\Omega} \sum_{n} \left[-(D - S\rho)(\tilde{\partial}_x \psi)(\tilde{\partial}_y \psi) - 2W(\tilde{\partial}_x \tilde{\partial}_y \psi)(\tilde{\nabla}^2 \psi) \right]. \qquad (17)$$

Fig. 7 shows the plot of Q_{xy} and σ_{xy} as a function of the shear strain γ for several values of $\overline{\rho}$. Here the shear rate is fixed as $\dot{\gamma} = 2 \times 10^{-4}$. In Fig. 8, we also plotted σ_{xy} for several values of $\dot{\gamma}$ fixing the total amount of surfactants as $\overline{\rho} = 0.1$. It is seen that both Q_{xy} and σ_{xy} initially increase rapidly and then decrease. We observed that the strain giving the peak position of Q_{xy} and σ_{xy} is almost constant, $\gamma_{\rm peak} \approx 2$, through the present simulation. On the other hand, the peak height of Q_{xy} is larger than that of σ_{xy} as a whole. $\overline{\rho}$ dependencies of the peak height of Q_{xy} and σ_{xy} are also different; the peak height of Q_{xy} increases linearly with $\overline{\rho}$, while that of σ_{xy} is almost independent of $\overline{\rho}$. However, a clear shear rate dependence of the peak height of σ_{xy} is observed in Fig. 8 as in Ref. (20).

6 Summary and Discussions

In this paper, using the CDS approach, we have investigated the effect of surfactants on the dynamics of phase separation between oil and water on the basis of newly proposed minimum two-order-parameter TDGL model. We

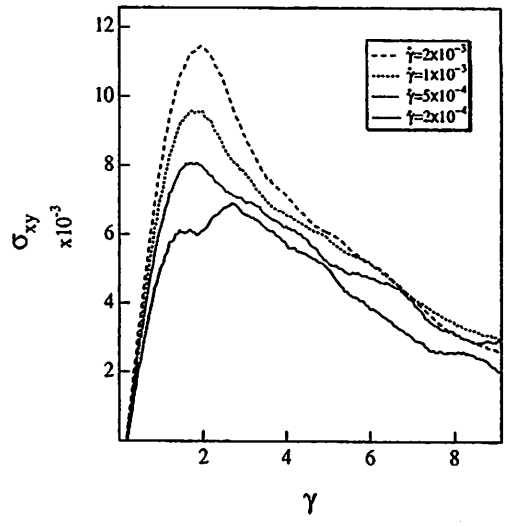

Figure 8: σ_{xy} (see Eq. (11)) as a function of the shear strain $\gamma = \dot{\gamma}t$ for fixed $\overline{\rho} = 0.1$ and $\dot{\gamma} = 2 \times 10^{-4}$, 5×10^{-4}, 1×10^{-3}, 2×10^{-3} from bottom to top.

restricted ourselves to the case where the volumes of water and oil are equal whereas the average surfactant concentration has been changed systematically. The time evolution of the typical length scale of the domains is characterized by an extremely slow dynamics. Our results can be interpreted according to the dynamical scaling assumption. Furthermore, we have investigated the dynamic response to the steady shear flow on bicontinuous microemulsions by changing the average surfactant concentration and the shear rate. As the surfactant concentration is increased, overshoot peak height of the anisotropic factor increases.

In the rest of this paper, we shall give some discussions. We first comment on the other possibilities of the two-order-parameter model. As regards the double-minimum local potential of ρ in Eq. (2), one may consider to replace it with a single-well potential ρ^2 which appears in the original model by Laradji *et al.* (see Eq. (1)). (The term $(\nabla^2\psi)^2$ is always necessary for the stability of the model.) We also examined this case, but it turned out that the system exhibits *macro*phase-separation rather than *micro*phase-separation within the parameter we investigated. This means that the surfactants do not adsorb enough at the interface to suppress the phase separation dynamics as far as $\rho(\nabla\psi)^2$ is the only included coupling term. This situation can be changed, for example, by including a local coupling term such as $\psi^2\rho$ according to the symmetry consideration. (Notice that $\psi^2\rho^2$ term in the model by Laradji *et al.* gives a higher order contribution than $\psi^2\rho$.) In this paper, we tried to reduce the number of different types of coupling terms as few as possible. We consider that the non-local coupling term used in this paper works more essentially for

the slow dynamics.

Finally we comment on the difference between the present rheological study based on the two-order-parameter model and the previous works (11; 12) which essentially utilize the single-order-parameter free energy proposed by Teubner and Strey to describe the microemulsion phase (23)

$$F_{\mathrm{TS}} = \int \mathrm{d}r \left[\mathcal{A}(\nabla^2\psi)^2 - \mathcal{B}(\nabla\psi)^2 + \mathcal{C}\psi^2\right], \tag{18}$$

where $\mathcal{A}, \mathcal{B}$ and $\mathcal{C}$ are positive constants ($\mathcal{B}$ is the surface tension parameter). This free energy is consistent with the observed scattering function which shows a peak at non-zero wavevector q and falls off as q^{-4} at large wavevectors. Since $\mathcal{C} > 0$ in Eq. (18), ψ locally prefers to vanish, $\psi \approx 0$, whereas ψ takes either $\psi \approx \pm\sqrt{a/2u} \neq 0$ for Eq. (2). (Notice that a in Eq. (2) is defined as positive.) In this sense, previous rheological studies of microemulsions (11; 12) have examined essentially the disordered phase as in the study of the rheology of block copolymer melts near to the critical point (24). In our work, on the other hand, we observe motions of domains with sharp oil/water interfaces, and hence dealing with dynamics of ordered phase. Similar approaches to the phase separating binary mixture (20) or the ordered block copolymers (25) have been also reported.

Acknowledgments

We would like to thank Dr. G. Gompper and Dr. J. L. Harden for their helpful discussions. We also thank Max-Planck-Institut für Kolloid und Grenzflächenforshungs for its hospitality while the part of this work was in progress. This work is supported by the Ministry of Education, Science and Culture, Japan (Grant-in-Aid for Scientific Research No. 08226233, No. 08740324 and No. 0657).

References

[1] G. Gompper and M. Schick, "*Self-Assembling Amphiphilic Systems*", Academic Press, (1994).

[2] M. Laguës and C. Sauterey, J. Phys. Chem. **84**, 3503 (1980); J. Peyrelasse and C. Boned, Phys. Rev. A **41**, 938 (1990).

[3] P. Guéring and B. Lindman, Langmuir **1**, 464 (1985); U. Olsson, K. Shinoda and B. Lindman, J. Phys. Chem. **90**, 4083 (1986); J-F. Bodet, J. R.

Bellare, H. T. Davis, L. E. Scriven and W. G. Miller, J. Phys. Chem. **92**, 1898 (1988).

[4] W. Jahn and R. Strey, J. Phys. Chem. **92**, 2294 (1988); P. K. Vinson, W. G. Miller, L. E. Scriven and H. T. Davis, J. Phys. Chem. **95**, 2546 (1991).

[5] see for instance, L. Auvray, "*Micelles, Membranes, Microemulsions, and Monolayers*", edited by W. M. Gelbart, D. Roux and A. Ben-Shaul, Springer, 347 (1994).

[6] M. Kotlarchyk, S. -H. Chen, J. S. Huang and M. W. Kim, Phys. Rev. Lett. **53**, 941 (1984).

[7] K. Kawasaki and K. Kawakatsu, Physica A **164**, 549 (1990); K. Kawakatsu and K. Kawasaki, *ibid.* **167**, 690 (1990).

[8] M. Laradji, O. G. Mouristen, S. Toxvaerd and M. J. Zuckermann, Phys. Rev. E **50**, 1243 (1994).

[9] M. Laradji, H. Guo, M. Grant and M. J. Zuckermann, J. Phys. A **24**, L629 (1991); J. Phys. Condens. Matter 4, 6715 (1992).

[10] G. Pätzold and K. Dawson, Phys. Rev. E **52**, 6908 (1995).

[11] C. J. Mundy, Y. Levin and K. A. Dawson, J. Chem. Phys. **97**, 7695 (1992).

[12] G. Pätzold and K. Dawson, J. Chem. Phys. **104**, 5932 (1996); Phys. Rev. E **54**, 1669 (1996).

[13] S. Komura and H. Kodama, Phys. Rev. E **55**, 1722 (1997).

[14] H. Kodama and S. Komura, J. de Physique II France **7**, 7 (1997).

[15] J. H. Schulman and J. B. Montagne, Ann. N.Y. Acad. Sci. **92**, 366 (1961).

[16] P. G. De Gennes and C. Taupin, J. Phys. Chem. **86**, 2294 (1982).

[17] T. Hashimoto and T. Izumitani, Macromolecules **26**, 3631 (1993); T. Izumitani and T. Hashimoto, Macromolecules **27**, 1744 (1994).

[18] Y. Oono and S. Puri, Phys. Rev. Lett. **58**, 836 (1987); Phys. Rev. A **38**, 434 (1988).

[19] S. Puri and Y. Oono, J. Phys. A **21**, L755 (1988).

[20] T. Ohta, H. Nozaki and M. Doi, Phys. Lett. **A145**, 304 (1990); J. Chem. Phys. **93**, 2664 (1990).

[21] A. Shinozaki and Y. Oono, Phys. Rev. E **48**, 2622 (1993).

[22] M. Laradji, H. Guo, M. Grant and M. J. Zuckermann, Phys. Rev. A **44**, 8184 (1991).

[23] M. Teubner and R. Strey, J. Chem. Phys. **87**, 3195 (1987).

[24] G. Fredrickson and R. G. Larson, J. Chem. Phys. **86**, 1553 (1987); A. Onuki, J. Chem. Phys. **87**, 3692 (1987).

[25] T. Ohta, Y. Enomoto, J. H. Harden and M. Doi, Macromolecules **26**, 4928 (1993); H. Kodama and M. Doi, Macromolecules **29**, 2652 (1996).